Evaluation of the ozone-related risk for winter wheat at local scale with the CRO_3PS model

L. Grünhage, H. Braden, J. Bender, S. Burkart, Y. Lehmann, M. Schröder

Abstract Tropospheric ozone poses a critical threat and a challenging problem to present and future, e.g. food security. In the recent years a stomatal flux-based risk evaluation methodology at leaf level was established in the context of the Convention on Long-Range Transboundary Air Pollution (LRTAP) for crops, forest trees and grasslands. According to the European Council Directive on ambient air quality and cleaner air for Europe local risk assessments for ozone have to be based on the parameters routinely measured by the European air quality monitoring networks. The SVAT model CRO_3PS provides a methodology for a local risk evaluation for winter wheat based on the critical level concept described in the actual, 2010 updated version of the LRTAP Convention's Mapping Manual. The exceedance of critical levels for wheat as well as potential losses of grain yield, grain mass and protein yield are calculated.

CRO_3PS – ein Modell zur Abschätzung potenzieller Ertragsverluste durch Ozon bei Winterweizen

Zusammenfassung Bodennahes Ozon stellt gegenwärtig und zukünftig u. a. eine Gefährdung für die Ertragsleistung landwirtschaftlicher Kulturpflanzen auch in Europa dar. In der vergangenen Dekade wurde im Rahmen des Genfer Luftreinhalteübereinkommens ein flussorientierter Ansatz auf Blattebene zur Beurteilung des Gefährdungsrisikos durch Ozon für landwirtschaftliche Nutzpflanzen, Waldbäume und Grünland erarbeitet. Gemäß der Richtlinie der Europäischen Gemeinschaft über Luftqualität und saubere Luft für Europa ist diese mittels ortsfester Messstationen zu überwachen. Das SVAT-Modell CRO_3PS parametrisiert ein Beurteilungsverfahren für potenzielle Ertragsverluste bei Weizen auf lokaler Ebene auf der Basis der critical levels (kritische Belastungswerte) und Fluss-Wirkung-Beziehungen, die in der 2010 aktualisierten Version des sog. Mapping Manual zum Genfer Luftreinhalteübereinkommen dokumentiert sind. Die Überschreitung der critical levels für Weizen werden berechnet sowie die potenziellen Verluste im Hinblick auf Kornertrag, Kornmassenertrag und Proteinertrag abgeschätzt.

Prof. Dr. Ludger Grünhage, Yvonne Lehmann, Matthias Schröder,
Institut für Pflanzenökologie, Justus-Liebig-Universität, Gießen.

Dr. Harald Braden,
Deutscher Wetterdienst, Abteilung Agrarmeteorologie, Zentrum für Agrarmeteorologische Forschung Braunschweig (ZAMF), Braunschweig.

Dr. Jürgen Bender,
Institut für Biodiversität, Johann Heinrich von Thünen-Institut (vTI), Braunschweig.

Dr. Stefan Burkart,
Institut für Agrarrelevante Klimaforschung, Johann Heinrich von Thünen-Institut (vTI), Braunschweig.

1 Introduction

A recent data synthesis, published by the ICP Vegetation Programme Coordination Centre[1], suggested widespread occurrence of ozone (O_3) effects on vegetation at ambient concentrations in Europe over the period 1990 to 2006 [1]. In principle, an ozone risk evaluation can be performed at the European/EMEP[2], at national as well as at local level. According to the Council Directives of the European Union the air quality has to be assessed and managed by means of sampling points for fixed measurement of ozone concentrations in our case [2 to 4]. In this context, local risk assessments for ozone have to be based on the parameters routinely measured by the European air quality monitoring networks.

This paper gives an overview of an O_3 risk assessment approach for winter wheat at local scale. The model CRO_3PS is based on the big-leaf model PLATIN (PLant-ATmosphere INteraction) [5; 6] and on the flux-based critical level concept developed by the members of the UNECE (United Nations Economic Commission for Europe) Working Group on Effects under the Convention on Long-Range Transboundary Air Pollution (LRTAP) [7]. It must be noted, that the measurement of all parameters needed for the LRTAP Convention's stomatal flux approach currently is not regulated by the Council Directives. The CRO_3PS model with documentation will be available for download at www.uni-giessen.de/cms/ukl-en/CRO3PS.

2 Theoretical background and the modular structure of the CRO_3PS model

The flux-based critical level approach is documented in the LRTAP Convention's Mapping Manual [7], assuming that the stomatal flux above a statistically deduced flux threshold Y provides an estimate of the critical amount of O_3 entering through the stomata and reaching the sites of action inside the plant. The statistically deduced flux threshold Y can be interpreted as a dummy for the O_3 detoxification capacity of the plants. The toxicologically relevant O_3 dose (POD, Phytotoxic Ozone Dose) is expressed as the cumulative stomatal uptake per unit projected leaf area (PLA) of the sunlit upper canopy leaves, i.e. the flag leaf in the case of wheat.

From experiments in open-top chambers performed in the 1980s/1990s a critical stomatal uptake of 1 mmol m^{-2} for relative wheat grain yield and a critical stomatal uptake of 2 mmol m^{-2} for relative wheat grain mass (e.g. 1 000 grain weight) and relative wheat protein yield was derived, taking into account a statistically deduced flux threshold of 6 nmol m^{-2} s^{-1} [7; 8]. The toxicologically relevant accumula-

[1] http://icpvegetation.ceh.ac.uk

[2] European Measurement and Evaluation Programme; www.emep.int

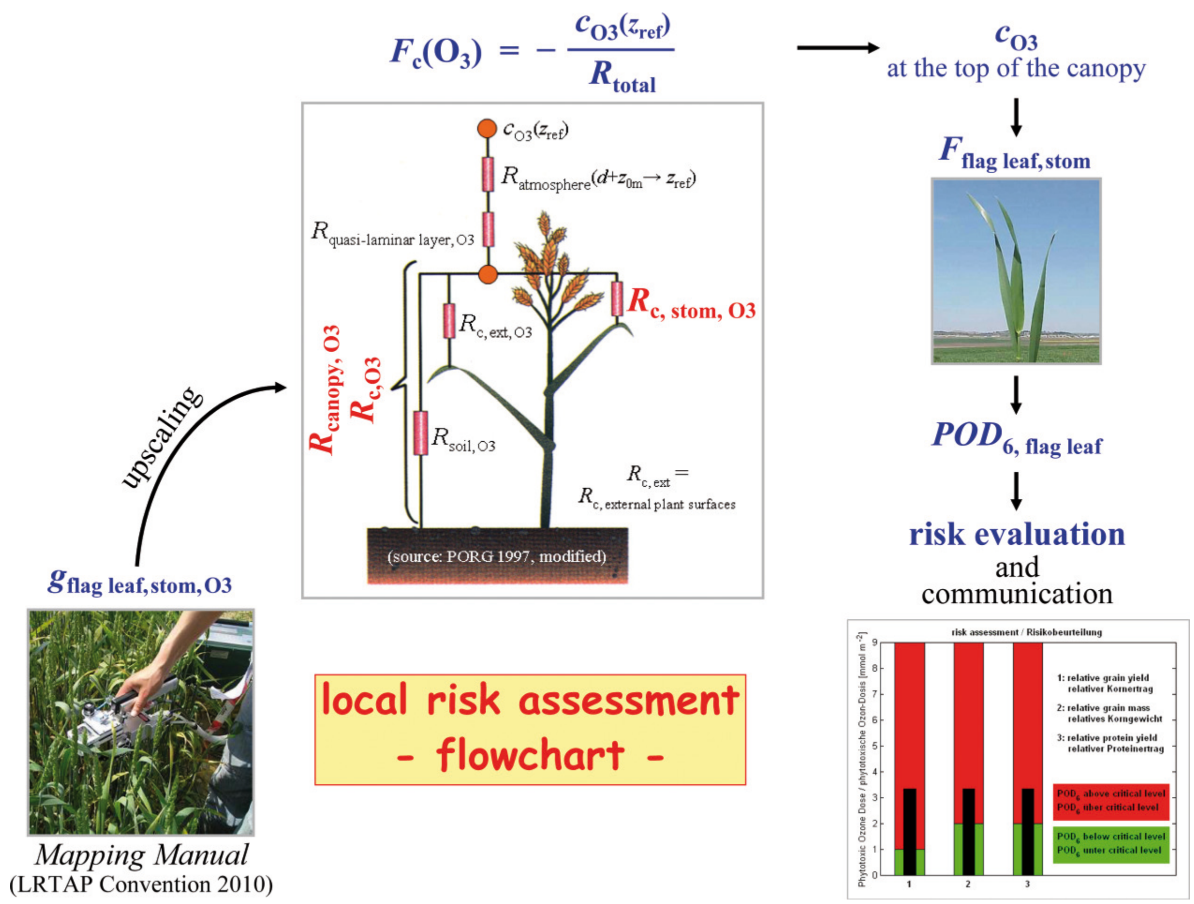

Figure 1. Flowchart for a local O_3 risk assessment for winter wheat.

tion period is based on thermal time accumulation and is defined as the time period 200 degree days before to 700 degree days after mid-anthesis. For details see [7] and [9].

The dependency of the flag leaf stomatal conductance on radiation, temperature and water budgets of the atmosphere (VPD, water vapour pressure deficit) and soil (PAW, plant available water content) as well as on the modifying influence of phenology and O_3 is parameterized according to a multiplicative Jarvis-Stewart approach:

$$g_{flag\ leaf,\ stom,\ O3} = g_{flag\ leaf,\ stom,\ max,\ O3} \cdot [\min(f_{phen}, f_{O3})] \cdot f_{light} \cdot \cdot \max\{f_{min}, (f_{temp} \cdot f_{VPD} \cdot f_{PAW})\} \quad (1)$$

where $g_{flag\ leaf,\ stom,\ max,\ O3}$ represents the maximum value of the stomatal conductance for O_3 (= 500 mmol O_3 m^{-2} PLA s^{-1}) and f_x weighting factors expressed in relative terms. The weighting factors f_x take values beween 0 and 1 as a proportion of $g_{flag\ leaf,\ stom,\ max,\ O3}$. For details of the flag leaf stomatal conductance parameterization see [7; 9].

The Mapping Manual's stomatal flux algorithm for wheat is based on the assumption that the O_3 concentration at the top of the canopy provides a reasonable estimate of the O_3 concentration at the upper surface boundary of the laminar boundary layer near the flag leaf, if the roughness sublayer near the canopy is not taken into account [7]:

$$F_{flag\ leaf,\ stom,\ O3} = c_{O3}(z_h) \cdot g_{flag\ leaf,\ stom,\ O3} \cdot \frac{R_{flag\ leaf,\ total,\ O3}}{R_{flag\ leaf,\ laminar\ layer,\ O3} + R_{flag\ leaf,\ total,\ O3}} \quad (2)$$

with

$F_{flag\ leaf,\ stom,\ O3}$	stomatal uptake by the flag leaf in $nmol \cdot m^{-2} \cdot s^{-1}$
$c_{O3}(z_h)$	O_3 concentration at canopy top h in $nmol \cdot m^{-3}$
$g_{flag\ leaf,\ stom,\ O3}$	stomatal conductance for O_3 in $m \cdot s^{-1}$
$R_{flag\ leaf,\ total,\ O3}$	total leaf resistance for O_3 in $s \cdot m^{-1}$
$R_{flag\ leaf,\ laminar\ layer,\ O3}$	resistance of the flag leaf laminar layer for O_3 in $s \cdot m^{-1}$

and

$$R_{flag\ leaf,\ total,\ O3} = \frac{1}{g_{flag\ leaf,\ stom,\ O3} + g_{flag\ leaf,\ external\ leaf\ surface,\ O3}} \quad (3)$$

with

$g_{flag\ leaf,\ external\ leaf\ surface,\ O3}$	conductance of the external leaf surface for O_3 in $m \cdot s^{-1}$ = $1/2{,}500\ m \cdot s^{-1}$

The resistance of the flag leaf laminar layer for O_3 is given by:

$$R_{flag\ leaf,\ laminar\ layer,\ O3} = 1.3 \cdot 150 \cdot \sqrt{\frac{L_{leaf}}{u(z_h)}} \quad (4)$$

with

L_{leaf}	characteristic crosswind leaf dimension in m; $L_{flag\ leaf}$ = 0.02 m
$u(z_h)$	horizontal wind velocity at canopy height h in $m \cdot s^{-1}$

The constant 150 exhibits the dimension $s^{0.5} \cdot m^{-1}$, where the factor 1.3 accounts for the differences in diffusivity between sensible heat and ozone.
Because O_3 concentrations are not measured at the canopy top by the European air quality monitoring networks, the O_3 concentrations measured at a reference height $z_{ref, O3}$ must be transformed to that at the top of the canopy. The conversion using the tabulated gradients published in the Mapping Manual yields unrealistic high accumulated stomatal fluxes. Therefore, the conversion has to be performed with an appropriate deposition model such as CRO_3PS.
Figure 1 summarizes the four steps of the stomatal flux-based risk assessment at local scale described in this paper:
(i) Upscaling the stomatal conductance of the flag leaf to canopy level
(ii) Modelling total O_3 flux and calculation of O_3 concentration at canopy top
(iii) Calculation of flag leaf stomatal uptake and Phytotoxic Ozone Dose (*POD*$_6$)
(iv) Risk evaluation

2 Upscaling the stomatal conductance of the flag leaf to canopy level

The flag leaf stomatal conductance $g_{\text{flag leaf, stom, O3}}$ is upscaled to canopy stomatal conductance $G_{\text{stom, O3}}$ by weighting with the one-sided leaf area index of the sunlit leaf fraction of the canopy and the ratio of the fractions of photosynthetically active radiation *PAR* intercepted by the total and the sunlit non-senescent leaves of the canopy (cf. eqs. (67) to (75) in [6]):

$$G_{\text{stom, O3}} = g_{\text{flag leaf, stom, O3}} \cdot \frac{1-\beta^*}{1-\beta^*_{\text{sunlit}}} \cdot LAI_{\text{sunlit}} \quad (5)$$

with LAI_{sunlit} the one-sided leaf area index of the sunlit leaf fraction of the canopy in $m^2 \cdot m^{-2}$ and (1-β*) and (1-β*$_{\text{sunlit}}$) the fraction of *PAR* intercepted by the total and the sunlit non-senescent leaves of the canopy, respectively.
The leaf area index of the sunlit leaf fraction of the canopy as well as the fraction of *PAR* intercepted by the canopy is parameterized by applying the sun-shade model of *de Pury* and *Farquhar* [10; 11]. Two parameters in the model have to be adapted to the actual winter wheat canopy structure: the beam *PAR* extinction coefficient and the modelled leaf scattering coefficient of *PAR*. The beam *PAR* extinction coefficient, which cannot be measured directly, can be derived from measurements of *LAI* and radiation profiles inside the canopy applying the Lambert-Beer law [11] (**Figure 2**). As shown in **Figure 3**, until growth stage „medium milk“ (BBCH code 75; cf. [12; 13]) the leaf scattering coefficient is 0.106, from growth stage „hard dough“ (BBCH code 87; cf. [12; 13]) onwards it can be parameterized by 0.37. We adjust the leaf scattering coefficient by comparison of measured and modelled albedo of *PAR*. Interestingly, the albedo of photosynthetically active and global radiation shows an inverse temporal development depending on canopy development (**Figure 4**). While the albedo of global radiation decreases after $DOY_{\text{BBCH 75}}$ (DOY, day of the year; from 0.33 to 0.20 at $DOY_{\text{BBCH 87}}$), the albedo of *PAR* increases (from 0.027 to 0.107 at $DOY_{\text{BBCH 87}}$). As illustrated in **Figure 5**, the photosynthetically active radiation absorbed by winter wheat canopies

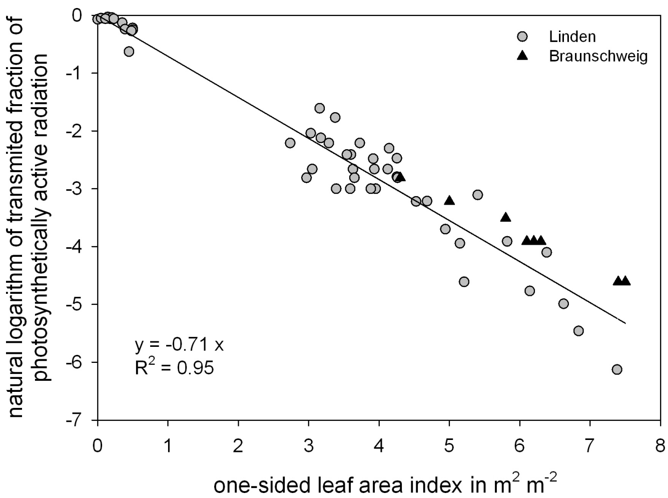

Figure 2. Natural logarithm of transmitted fraction of photosynthetically active radiation ($PAR_{\text{soil surface}}$/ $PAR_{\text{canopy top}}$) vs. leaf area index.
Winter wheat fields in Braunschweig and Linden near Gießen; week before growth stage BBCH 39 (cf. Table) to harvest and in autumn 2009

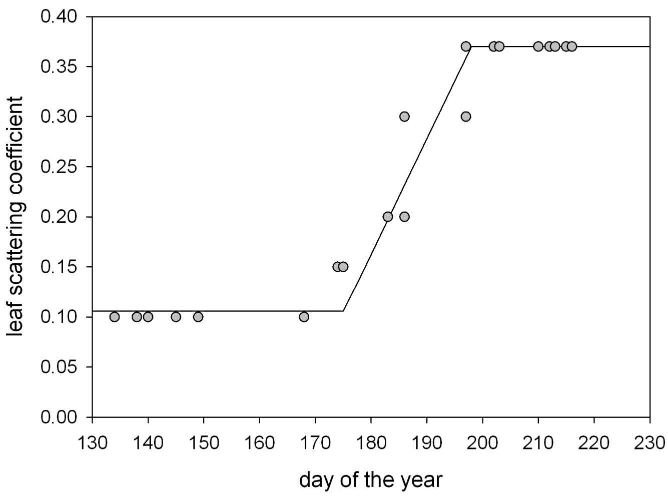

Figure 3. Modelled leaf scattering coefficient of photosynthetically active radiation.
Winter wheat fields in Linden near Gießen; week before growth stage BBCH 39 (cf. Table) to harvest in 2009

could be modelled quite well with the adjusted sun-shade model.
Additionally, the upscaling approach and the parameterization of total O_3 flux (see section 3) presuppose the simulation of the temporal development of the winter wheat canopy. The temporal development of leaf area index *LAI* for non-senescent and senescent leaves as well as of canopy height *h* is calculated by algorithms adopted from the well-validated agrometeorological model for estimation of actual evapotranspiration AMBAV (Agrarmeteorologisches Modell zur Berechnung der aktuellen Verdunstung) of the German Meteorological Service [14; 15]. AMBAV describes the development of *LAI* and *h* as a function of the day of the year (DOY) depending on characteristic growth stages routinely observed by the German phenological network. The actual parameterization for *LAI* and *h* is given in [16]. If the growth stages needed are not observed, they can be estimated by growing degree-days *GDD*, i.e. by accumulation of mean daily temperatures above a base temperature of 0 °C starting at day 60 of the respective year (**Table**; temperature sums

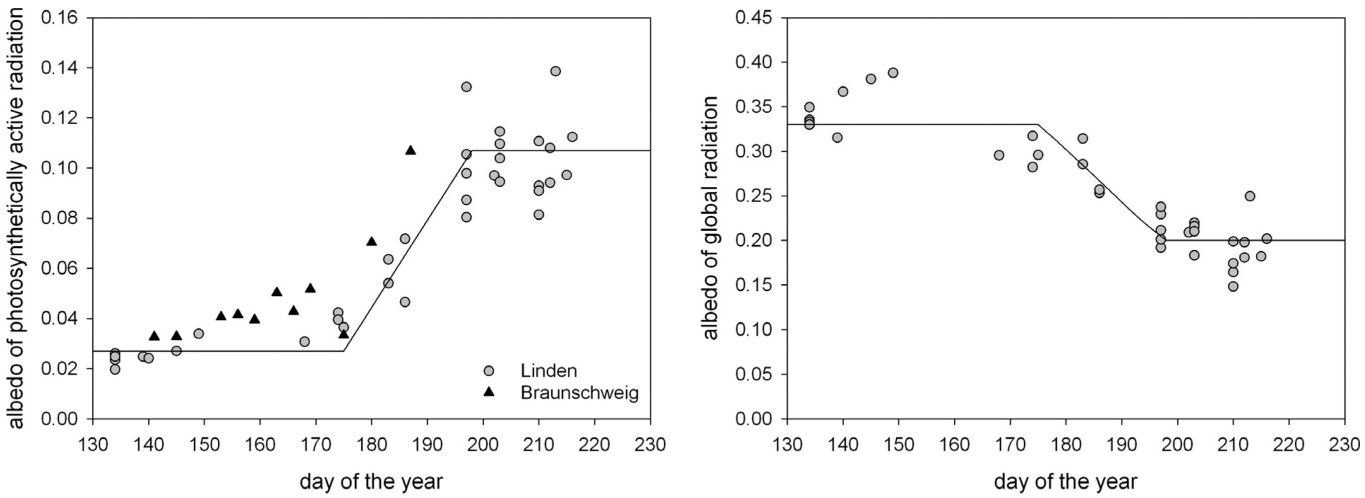

Figure 4. Measured and modelled albedo of photosynthetically active and global radiation.
Winter wheat fields in Braunschweig and Linden near Gießen; week before growth stage BBCH 39 (cf. Table1) to harvest in 2009

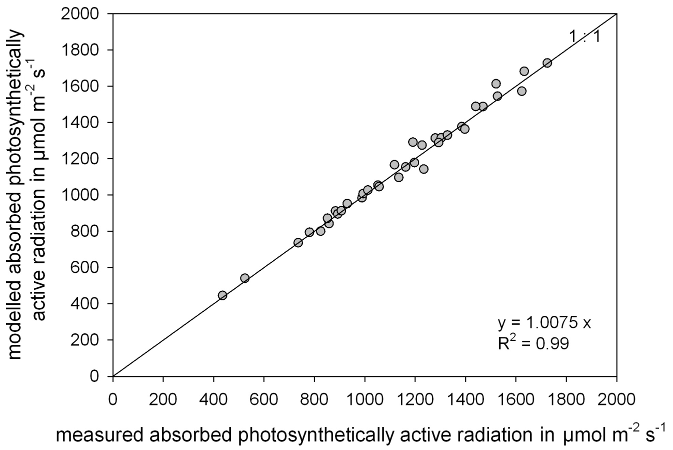

Figure 5. Modelled vs. measured absorbed photosynthetically active radiation.
Winter wheat fields in Linden near Gießen; week before growth stage BBCH 39 (cf. Table1) to harvest in 2009

derived from data of Braunschweig, Laupheim, Linden and Lüchow).

In principle, any upscaling procedure from leaf to canopy stomatal conductance has to be validated by means of evapotranspiration measurements via e.g. weighable backfilled lysimeters, canopy gas exchange chambers or eddy covariance measurements. As illustrated in **Figure 6**, the CRO_3PS upscaling approach delivers canopy stomatal conductance values which agree well with values measured with the portable gas exchange chamber system described in [19].

3 Modelling total O_3 flux and calculation of O_3 concentration at canopy top

The O_3 concentration at the top of the canopy is a function of the transport properties of the atmosphere near the canopy and of the sink properties of the canopy. Modelling the underlying processes requires a more or less extensive reduction of their complexity. The degree of simplification depends on what is to be modelled and on the availability of data to operate the model. As mentioned above, the CRO_3PS model presented here is based on the SVAT model PLATIN [5; 6]. Like numerous other SVAT models PLATIN is based on the big-leaf concept which replaces the vertical resolution of sources and sinks within the plant stand (including the soil surface beneath) by the idea of a single big leaf with overall properties equivalent to those of the complete plant/soil-surface system. The core module of PLATIN is based on the canopy energy budget and calculates the exchange of sensible and latent heat between phytosphere and near-surface atmosphere. Coupled to this the exchange of trace gases and fine-particle constituents is quantified. The vertical transport between an above-canopy reference height z_{ref}, for

Encoding of characteristic growth stages of winter wheat.
DOY = day of the year; GDD = growing degree-days, baseline 0 °C

growth stages		GDD
DOY_{start}	60	
$DOY_{BBCH\ 31}$ *)	stem elongation, first node at least 1 cm above tillering node	398
$DOY_{between}$	$DOY_{BBCH\ 31}$ – 5	
$DOY_{BBCH\ 39}$	flag leaf stage: flag leaf fully unrolled, ligule just visible	732
$DOY_{BBCH\ 51}$	beginning of heading: tip of inflorescence emerged from sheath, first spikelet just visible	869
DOY_{max}	$DOY_{BBCH\ 51}$ + 5	
$DOY_{BBCH\ 65}$	mid-anthesis – full flowering: 50 % of anthers mature	1024
$DOY_{BBCH\ 75}$	medium milk: grain content milky, grains reached final size, still green	1345
$DOY_{BBCH\ 87}$	hard dough: grain content solid. Fingernail impression held	1724
$DOY_{harvest}$	over-ripe: grain very hard, cannot be dented by thumbnail or harvest by harvester-thresher	1994

*) after [12; 13], according to [17; 18]

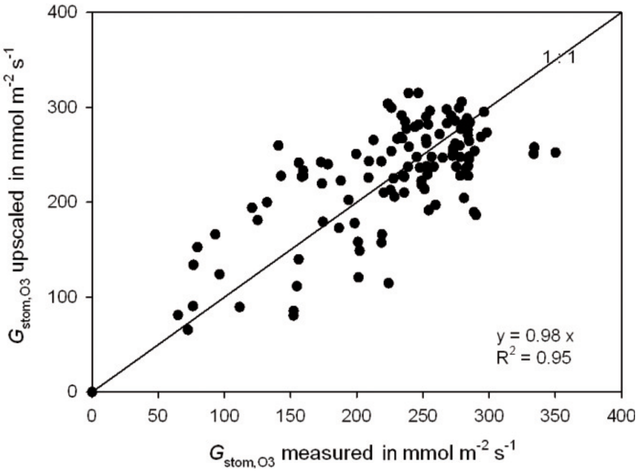

Figure 6. Portable gas exchange chamber system and upscaled vs. measured canopy stomatal conductance.
Winter wheat field in Braunschweig; comparison period: 2009-06-06 to 2009-06-17, 11 am to 4 pm CET

which air properties and concentrations of matter must be known, and the sinks and/or sources of the plant/soil-surface system is modelled using three resistances: (1) the turbulent atmospheric transport resistance R_{ah} in $s \cdot m^{-1}$ between reference height and the level of momentum sink ($z = d + z_{0m}$; d: displacement height, z_{0m}: roughness length for momentum); (2) the quasi-laminar resistance R_b in $s \cdot m^{-1}$ between momentum-sink level and the surface of the big leaf to account for the differences between momentum transfer and transport of energy and matter; and (3) the canopy resistance R_c in $s \cdot m^{-1}$ which in turn is modelled using a number of further resistances arranged in series and in parallel.

The exchange of O_3 between the phytosphere and the atmosphere near the ground can be modelled by:

$$F_{c,\,total}(O_3) = -\frac{\rho_{O3}(z_{ref,\,O3})}{R_{ah}(d + z_{0m}, z_{ref,\,O3}) + R_{b,O3} + R_{c,O3}} \quad (6)$$

with

$F_{c,total}(O_3)$ total vertical atmosphere-canopy flux of O_3 in $\mu g \cdot m^{-2} \cdot s^{-1}$

$\rho_{O3}(z_{ref,\,O3})$ measured O_3 concentration at reference height $z = z_{ref,\,O3}$ in $\mu g \cdot m^{-3}$

If the roughness sublayer is not considered, the resistance of the atmosphere between O_3 concentration measurement height and the upper surface boundary of the quasi-laminar layer can be calculated after eq. (2) in [6], and the resistance of the quasi-laminar layer for O_3 after eq. (7) in [6] taking into account the respective value for $(Sc_{O3}/Pr)^{2/3}$ (= 1.19; cf. Table 2 in [6]).

The actual canopy resistance for O_3 is the reciprocal canopy conductance which is the sum of stomatal and non-stomatal canopy conductance. Canopy stomatal conductance $G_{stom,\,O3}$ is derived by upscaling the flag leaf stomatal conductance (section 2), the non-stomatal canopy conductance $G_{non\text{-}stom,\,O3}$ is estimated according to [20].

$$G_{c,\,non\text{-}stom,\,O3} = g_{flag\ leaf,\ external\ leaf\ surface,\ O3} \cdot LAI_{total} + \frac{1}{R_{inc} + R_{soil}} \quad (7)$$

with $R_{inc} = b \cdot LAI_{total} \cdot h \cdot u_*^{-1}$ with $b = 14\ m^{-1}$ and $R_{soil} = 200\ s \cdot m^{-1}$.

u_* is the friction velocity which is calculated according to eq. (4) in [6]. The O_3 concentration at canopy top is calculated according to eq. (60) in [6]:

$$\rho_{O3}(h) = \rho_{O3}(z_{ref,\,O3}) + [F_{c,\,total}(O_3) \cdot R_{ah}(h, z_{ref,O3})] \quad (8)$$

Because rootzone plant available soil water content PAW in % is not measured by the air quality monitoring networks, it is approximated applying a simple soil water balance „bucket“ model. Actual PAW is given by:

$$PAW = \min\left\{\max\left(0, \frac{SW - SW_w}{SW_c - SW_w} \cdot 100\right), 100\right\} \quad (9)$$

with

SW actual soil water content of the rootzone in mm

SW_c soil water content of the rootzone at field capacity in mm

SW_w soil water content of the rootzone at permanent wilting point in mm

As described in the LRTAP Convention's Mapping Manual [7] the influence of PAW on stomatal behaviour is parameterized according to [21]:

$$f_{PAW} = 1 \quad \text{if} \quad PAW_t \le PAW \le 100\,\%$$
$$f_{PAW} = 1 + \frac{PAW - PAW_t}{PAW_t} \quad \text{if} \quad PAW < PAW_t \quad (10)$$

with PAW_t is the threshold PAW of 50% above which relative stomatal conductance it as maximum, i.e. unity (cf. [7; 9]). According to expert knowledge of the German Agrometeorological Service PAW is calculated for the top 0.6 m of the soil for a loamy sand (German classification Su2, schwach schluffiger Sand) with a field capacity of 0.25 $m^3\ m^{-3}$, a permanent wilting point of 0.06 $m^3\ m^{-3}$ and an effective rooting zone of 0.8 m (at growth stage BBCH 31 roots reach 0.7 m depth, at BBCH 39 roots reach 0.8 m depth) [22]. Changes in soil water content SW in mm over a given time in the effective rooted zone is estimated through a simple mass balance equation:

$$SW_i = \min(SW_c, SW_{i-1} - E_{i-1} + W_{in,i} + CR_i) \quad (11)$$

with
E evapotranspiration in mm
W_{in} amount of precipitation and/or dew reaching the soil surface in mm
CR capillary rise in mm
Because the soil water module is parameterized for the top 0.6 m of the soil only, eq. (11) has to be modified from growth stage BBCH 31 onwards when effective rooted zone exceeds the top 0.6 m:

$$SW_i = \min(SW_c, SW_{i-1} - \text{evapofactor} \cdot E_{i-1} + W_{in,i} + CR_i) \quad (12)$$

For the time period "$DOY_{BBCH31} \leq DOY < DOY_{BBCH39}$" evapofactor is 0.95 if $PAW < PAW_t$, otherwise evapofactor is 1. For the time period "$DOY \geq DOY_{BBCH39}$" evapofactor takes the following values: 0.95 if $PAW_t - 10 \leq PAW < PAW_t$ and 0.90 if $PAW < PAW_t - 10$. Otherwise evapofactor is 1.
Because the soil layer "0 - 0.3 m" is drying-out faster than the deeper "0.3 - 0.6 m" layer, the Jarvis-Stewart function for PAW was extended by an additional factor:

$$f_{PAW} = \max\left(0, \left\{1 + \left[(PAW - PAW_t) \cdot \frac{\mathrm{PAW_{factor}}}{PAW_t}\right]\right\}\right) \quad \text{if } PAW < PAW_t \quad (13)$$

with $PAW_{factor} = 1.25$.
The soil water module was calibrated against AMBAV with the 2003 data set of a non-irrigated and validated with the 2003 data set of an irrigated winter wheat field. As illustrated in **Figure 7** CRO_3PS models the plant available soil water content as well as the evapotranspiration rates adequately.
It must be noted that the parameters of the Jarvis-Stewart function for temperature as described in [7; 9] ($T_{min,\,flag\,leaf}$ = 12 °C, $T_{opt,\,flag\,leaf}$ = 26 °C, $T_{max,\,flag\,leaf}$ = 40 °C) has to be adapted to canopy level ($T_{min,\,canopy}$ = 0 °C, $T_{opt,\,canopy}$ = 20 °C, $T_{max,\,canopy}$ = 40 °C) because a wheat canopy is physiologically active below a temperature of 12 °C.

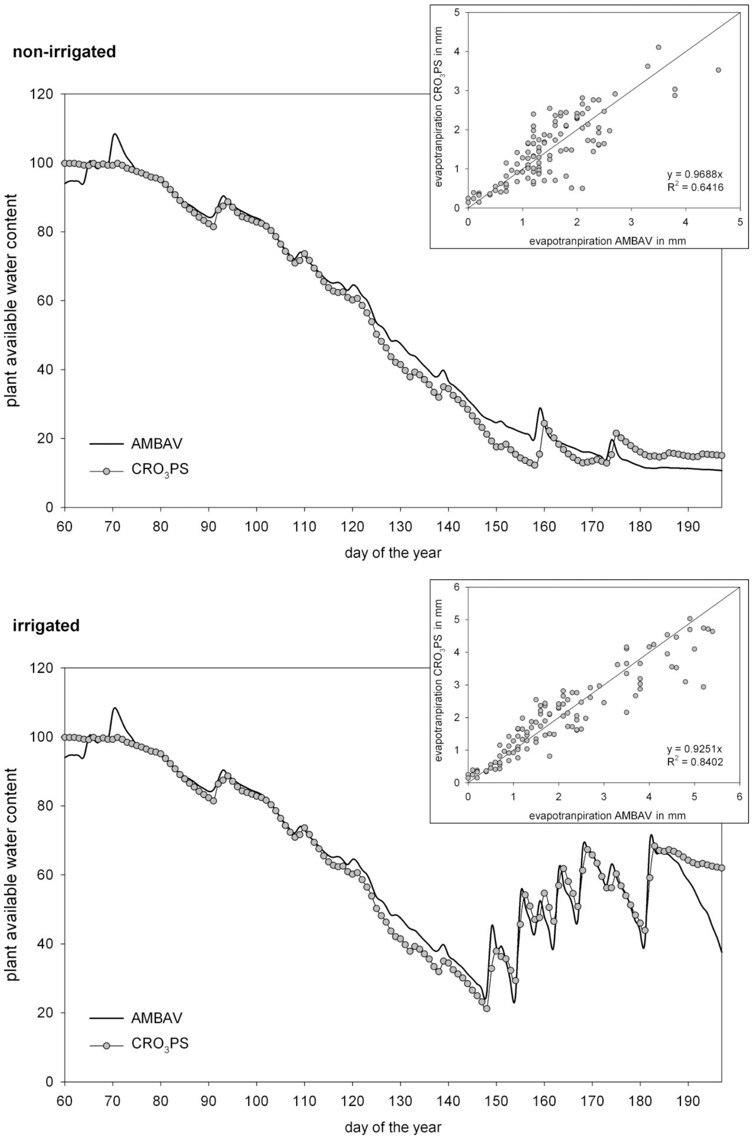

Figure 7. Plant available soil water content and evapotranspiration of a non-irrigated and an irrigated winter wheat field in 2003.

4 Calculation of flag leaf stomatal uptake and Phytotoxic Ozone Dose (POD_6)

Flag leaf stomatal uptake during the toxicologically relevant accumulation period from 200 degree-days before to 700 degree-days after mid-anthesis is calculated during daylight hours (global radiation > 50 W m^{-2}) according to eq. (2). The Phytotoxic Ozone Dose above the flux threshold of 6 nmol m^{-2} s^{-1} is given by:

$$POD_6 = \sum_{i=1}^{n}\left[\left(\max\left(F_{\text{flag leaf, stom, O3}} - 6, 0\right)\right) \cdot \Delta t\right]_i \quad (14)$$

where n denotes the number of daylight hours included in the toxicologically relevant accumulation period.

5 Risk evaluation

CRO_3PS allows a risk evaluation for two soil moisture conditions: (1) a risk evaluation for a situation with no soil water limitation on stomatal behaviour, i.e. $f_{PAW} = 1$ which can be interpreted as a worst-case assessment; and (2) a risk evaluation under "actual" soil water content (not groundwater influenced), i.e. the soil water content is a function of amount and distribution of precipitation and of evapotranspiration. The two cases margin the range of potential POD_6 and yield losses in a respective year due to soil water content and weather conditions.
Potential yield losses can be estimated via stomatal flux-effect relations for relative grain yield, grain mass and protein yield [7; 9]:

$$\text{relative grain yield} = 1.00 - 0.038 \cdot POD_6 \quad (15)$$
$$\text{relative grain mass} = 1.00 - 0.033 \cdot POD_6 \quad (16)$$
$$\text{relative protein yield} = 1.01 - 0.025 \cdot POD_6 \quad (17)$$

An example of a local worst-case risk evaluation ($f_{PAW} = 1$) for relative grain yield is given in **Figure 8** for the monitoring station Radebeul-Wahnsdorf of the air quality monitoring network in Saxony, Germany. From the mid 1980s onwards

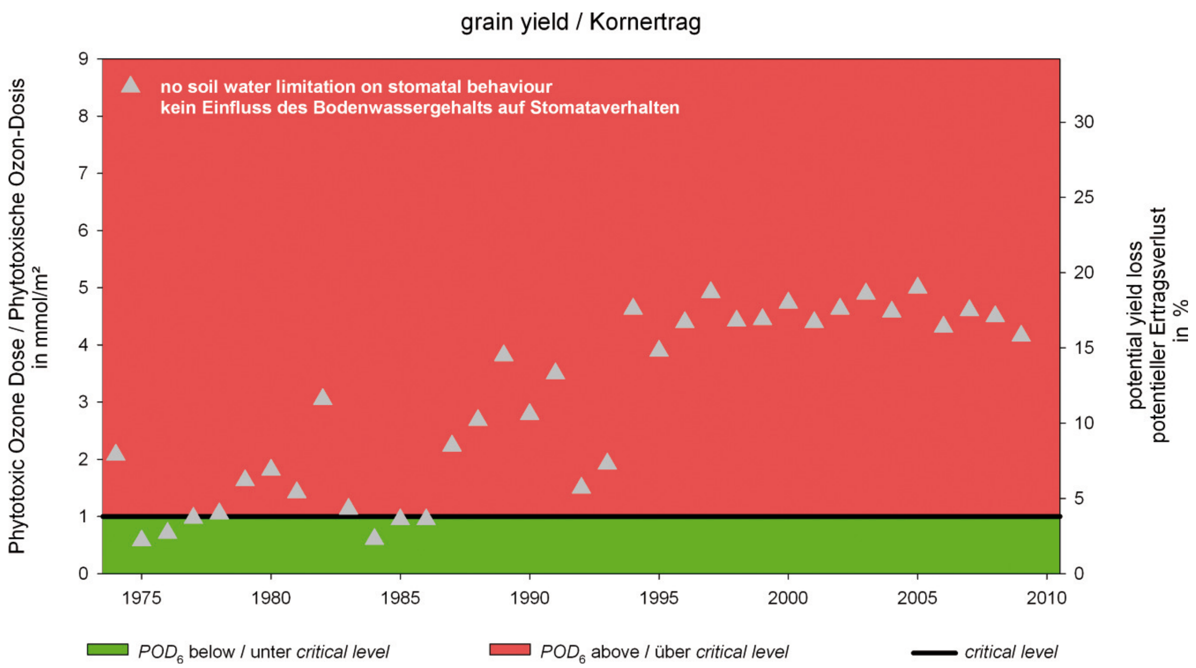

Figure 8. Phytotoxic Ozone Dose (*POD_6*) and potential grain yield loss for Radebeul-Wahnsdorf, Saxony. Worst-case risk evaluation according to the LRTAP Convention's Mapping Manual [7].
Data source: O_3 concentration – air quality monitoring network Saxony, meteorological data – monitoring station Dresden-Klotzsche of the German Weather Service

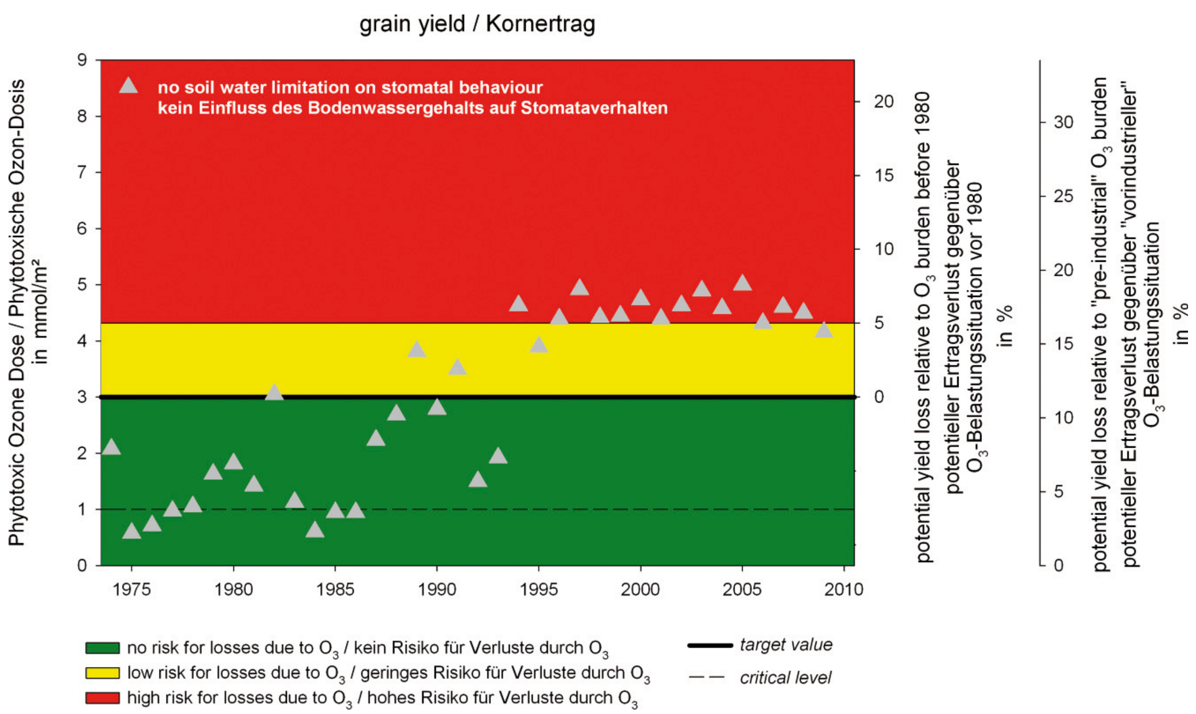

Figure 9. Phytotoxic Ozone Dose (*POD_6*) and potential grain yield loss for Radebeul-Wahnsdorf, Saxony. Worst-case risk evaluation according to the LRTAP Convention's Mapping Manual [7] and the recommendations of the working group NA 134-03-03-02 "Effects of Air Pollutants on Vegetation" of the Commission on Air Pollution Prevention of VDI and DIN – Standards Committee KRdL [23].
Data source: O_3 concentration – air quality monitoring network Saxony, meteorological data – monitoring station Dresden-Klotzsche of the German Weather Service

the critical level of 1 mmol m^{-2} for relative wheat grain yield is exceeded every year (up to a factor of 5) and relative grain yield losses between 15 and 20% are estimated since 1995. A continuative interpretation is suggested by the working group NA 134-03-03-02 "Effects of Air Pollutants on Vegetation" of the Commission on Air Pollution Prevention of VDI and DIN – Standards Committee KRdL [23]. At first, from the information given in the LRTAP Convention's Mapping Manual [7] it can be deduced that the estimated potential yield losses calculated according to eqs. (15) to (17) are relative to "pre-industrial" O_3 burden. Secondly, as mentioned above the stomatal flux-effect relationships underlying experiments were conducted in the 1980s/1990s. Due to comparison of ambient O_3 concentration levels during this time and related potential yield losses (e.g. Figure 8) it seems to be adequate to define a *POD_6* target value within the meaning of Article 2 of the European Council Directive 2008/50/EC [4]. The working group NA 134-03-03-02 recommends a *POD_6*

target value of 3 mmol m^{-2} which is interpreted as the upper margin of the O_3 burden before 1980. Relative yield losses should be related to this target value and the use of a three colour scale (traffic lights) is recommended to indicate and communicate the degree of risk for ozone injury as illustrated in **Figure 9**. The results of this worst-case evaluation for Radebeul-Wahnsdorf showed a clear increase in the risk for yield loss from the mid 1970s to 2010 with a high risk for losses due to O_3 during the last 15 years.

Acknowledgements

We would like to thank the Saxon State Agency for Environment, Agriculture and Geology (LfULG) and the German Weather Service for providing the ozone and meteorological data, respectively.

References

[1] *Hayes, F.; Mills, G.; Harmens, H.; Norris, D.*: Evidence of widespread ozone damage to vegetation in Europe. Bangor, UK: ICP Vegetation Programme Coordination Centre, Centre for Ecology & Hydrology (2007). http://icpvegetation.ceh.ac.uk

[2] Council Directive 96/62/EC of 27 September 1996 on ambient air quality assessment and management. OJ EC (1996) No. L 296, p. 55-63.

[3] Directive 2002/3/EC of the European Parliament and of the Council of 12 February 2002 relating to ozone in ambient air. OJ EC (2002) No. L 67, p. 14-30.

[4] Directive 2008/50/EC of the European Parliament and of the Council of 21 May 2008 on ambient air quality and cleaner air for Europe. OJ EU (2008) No. L 152, p. 1-44.

[5] *Grünhage, L.; Haenel, H.-D.*: PLATIN (PLant-ATmosphere INteraction) I: a model of plant-atmosphere interaction for estimating absorbed doses of gaseous air pollutants. Environm. Pollut. 98 (1997), p. 37-50.

[6] *Grünhage, L.; Haenel, H.-D.*: Detailed documentation of the PLATIN (PLant-ATmosphere INteraction) model. Landbauforsch. Volk. special issue 319 (2008), p. 1-85. www.uni-giessen.de/cms/ukl-en/PLATIN

[7] LRTAP Convention, 2010: Mapping Manual 2004. Manual on methodologies and criteria for modelling and mapping critical loads & levels and air pollution effects, risk and trends. Chapter 3. Mapping critical levels for vegetation. 2010 revision. http://icpvegetation.ceh.ac.uk

[8] *Mills, G.; Pleijel, H.; Braun, S.; Büker, P.; Bermejo, V.; Danielsson, H.; Emberson, L.; Grünhage, L.; González Fernández, I.; Harmens, H.; Hayes, F.; Karlsson, P.-E.; Simpson, D.*: New stomatal flux-based critical levels for ozone effects on vegetation. Atmos. Environm. submitted.

[9] *Grünhage, L.; Pleijel, H.; Mills, G.; Bender, J.; Danielsson, H.; Lehmann, Y.; Castell, J.-F.; Bethenod, O.*: Parameterisation of flag leaf stomatal conductance for ozone flux modelling in wheat. Atmos. Environm. submitted.

[10] *de Pury, D. G. G.; Farquhar, G .D.*: Simple scaling of photosynthesis from leaves to canopies without the errors of big-leaf models. Plant Cell Environm. 20 (1997), p. 537-557.

[11] *Grünhage, L.; Haenel, H.-D.*: Detailed documentation of the PLATIN (PLant-ATmosphere INteraction) model. Appendix B – improved radiation model. www.uni-giessen.de/cms/ukl-en/PLATIN

[12] *Meier, U.*(ed.): Growth stages of mono- and dicotyledonous plants. BBCH Monograph, 2nd ed. Braunschweig: Federal Biological Research Centre for Agriculture and Forestry 2001. www.jki.bund.de/fileadmin/dam_uploads/_veroeff/bbch/BBCH-Skala_englisch.pdf

[13] *Meier, U.*: Phenological growth stages. In: *Schwartz, M. D.* (Ed.): Phenology: an integrative environmental science; p. 269-283. Dordrecht: Kluwer 2003.

[14] *Löpmeier, F.-J.*: Agrarmeteorologisches Modell zur Berechnung der aktuellen Verdunstung (AMBAV). Beiträge zur Agrarmeteorologie 7. Offenbach: Deutscher Wetterdienst 1983.

[15] *Löpmeier, F.-J.*: Berechnung der Bodenfeuchte und Verdunstung mittels agrarmeteorologischer Modelle. Z. Bewässerungswirtsch. 29 (1994), p. 157-167.

[16] *Grünhage L.; Braden, H.; Lehmann, Y.; Löpmeier, F.-J.*: Parameterization of winter wheat canopy development. www.uni-giessen.de/cms/ukl-en/PLATIN

[17] *Zadoks, J. C.; Chang, T. T.; Konzak, C. F.*: A decimal code for the growth stages of cereals. Weed Res. 14 (1974), p. 415-421.

[18] *Tottman, D. R.*: The decimal code for the growth stages of cereals, with illustrations. Ann. Appl. Biol. 110 (1987), p. 441-454.

[19] *Burkart, S.; Manderscheid, R.; Weigel, H.-J.*: Design and performance of a portable gas exchange chamber system for CO_2- and H_2O-flux measurements in crop canopies. Environm. Exp. Bot. 61 (2007), p. 25-34.

[20] *Simpson, D.; Fagerli, H.; Jonson, J. E.; Tsyro, S.; Wind, P.; Tuovinen, J.-P.*: Transboundary acidification, eutrophication and ground level ozone in Europe. EMEP Status Report 1, Part I: Unified EMEP model description. Oslo: Norwegian Meteorological Institute 2003.

[21] *Sadras, V. O.; Milroy, S. P.*: Soil-water thresholds for the responses of leaf expansion and gas exchange: A review. Field Crop Res. 47 (1996), p. 253-266.

[22] Bodenkundliche Kartieranleitung. Hrsg.: Ad-hoc-AG Boden. 5. Aufl. Stuttgart: E. Schweizerbart 2005.

[23] *Grünhage, L.; Bender, J.; Jäger, H.-J.; Matyssek, R.; Weigel, H.-J.*: Beurteilungswerte für Ozon zum Schutz der Vegetation. Gefahrstoffe – Reinhalt. Luft 71 (2011) No. 3, p. 79-89.